Cluster Formation in a Granular Medium Fluidized by Vibrations in Low Gravity

Éric Falcon,[1,*] Régis Wunenburger,[2] Pierre Évesque,[3] Stéphan Fauve,[1] Carole Chabot,[2]
Yves Garrabos,[2] and Daniel Beysens[4]
[1]*Laboratoire de Physique Statistique, École Normale Supérieure, 24 rue Lhomond, 75 005 Paris, France*
[2]*Institut de Chimie et de la Matière Condensée de Bordeaux, avenue du Docteur A. Schweitzer, 33 608 Pessac, France*
[3]*Laboratoire M.S.2M., École Centrale Paris, 92 295 Chatenay-Malabry Cedex, France*
[4]*D.R.F.M.C., Commissariat à l'Énergie Atomique Grenoble, 38 054 Grenoble Cedex 9, France*
(Received 24 November 1998)

We report an experimental study of a "gas" of inelastically colliding particles, excited by vibrations in low gravity. In the case of a dilute granular medium, we observe a spatially homogeneous gaslike regime, the pressure of which scales like the $3/2$ power of the vibration velocity. When the density of the medium is increased, the spatially homogeneous fluidized state is no longer stable but displays the formation of a motionless dense cluster surrounded by low particle density regions.

PACS numbers: 45.70.–n, 81.70.Ha, 83.10.Pp, 83.70.Fn

Vibrated granular media display striking fluidlike properties: convection and heaping [1,2], period doubling instabilities [3], and parametric extended [4] or localized [5] surface waves. When the vibration is strong enough, the granular medium undergoes a transition to a fluidized state. It looks like a gas of particles that can be described using kinetic theory [6]. The "granular temperature," i.e., the mean kinetic energy per particle, is determined by the balance between the power input due to the external vibration and dissipation by inelastic collisions. Fluidization by vibrations has been studied experimentally [7,8] and numerically [8,9], but no agreement has been found so far for the dependence of the granular temperature on the amplitude and the frequency of external vibrations [10–12].

One of the most interesting properties of such "granular gases" is the tendency to form clusters. Although this has probably been known since the early observation of planetary rings [13], there exist only a few recent laboratory experiments. One experiment, with a horizontally shaken two-dimensional layer of particles, displayed a cluster formation, but the coherent friction force acting on all the particles was far from being negligible [14]. We performed a similar three-dimensional experiment in the laboratory and observed clustering, but we could not rule out the possibility of a resonance mechanism between the time of flight under gravity and the excitation frequency [15]. Various cluster types in granular flows have also been observed numerically [16]. The mechanisms of cluster formation are an active subject of research that still deserves more study because of its relevance to technical, astrophysical [17], or geophysical [18] applications of granular media. At a more fundamental level, it is of a primary interest to understand the new qualitative behaviors due to inelasticity of collisions, i.e., nonconservation of energy, in kinetic theory.

In this Letter, we report a study of the kinetic regimes of a granular medium, fluidized by vibrating its container in a low gravity environment. The motivation for low gravity is to achieve an experimental situation in which inelastic collisions are the only interaction mechanism. The aim of the experiment is to observe new phenomena which result from the inelasticity of the collisions and are thus absent in a usual gas. In the dilute case, we show that the pressure of a granular gas scales like the $3/2$ power of the vibration velocity. When the density of the medium is increased, we observe for the first time that an ensemble of solid particles in erratic motion interacting only through inelastic collisions can generate the formation of a motionless dense cluster.

The *Mini-Texus 5* space probe was launched from Esrange (Northern Sweden) on a Nike-Improved Orion rocket with three cubic containers on board, 1 cm^3 in inner volume, with clear sapphire walls. Each cell is filled, respectively, with 0.281, 0.562, and 0.8915 g of 0.3–0.4 mm in diameter bronze spheres (solid fractions: 3.2%, 6.4%, and 10.1%). Thus, the total number of particles in each cell is about 1420, 2840, and 4510, respectively, corresponding to roughly 1, 2, and 3 particle layers at rest. An electrical motor, with eccentric transformer from rotational to translational motion, drives the vessels sinusoidally at frequency f and maximal displacement amplitude A in the ranges 1 to 60 Hz and 0.1 to 2.5 mm, respectively. The vibrational parameters during the time line are listed in Table I. Motion of particles is visualized and recorded by an SWM039 CCD camera, fixed in the frame of the space probe, that captures 742×582 pixel images with an 40 ms exposure time. Each cell is illuminated by a light-emitting diode at a right angle to the observation during 1 ms with a frequency detuning of 2 Hz with respect to the drive signal. Accelerations are measured by piezoelectric accelerometers (PCB 356A08) screwed in the shaft in a triaxial way. Typical output sensitivities in the vibrational direction and in the perpendicular directions are, respectively, 0.1 and 1 V/g, with $g = 9.81\ m\,s^{-2}$ the acceleration of gravity. A piezoelectric pressure sensor (PCB 106B50), 1.53 cm in diameter, is fixed on the "top" of each cell. The accelerometer orientation, in the direction of vibration, is such that

 0031-9007/99/83(2)/440(4)$15.00 © 1999 The American Physical Society

TABLE I. Vibrational parameters during the 200 s of low gravity. Time segment is the duration of each experiment at fixed amplitude and frequency without taking into account the transient states. $V = 2\pi A f$ and $\Gamma = 4\pi^2 A f^2/g$ are, respectively, the velocity amplitude and the dimensionless acceleration amplitude of the vessels. Data from experiment 1 had a poor signal-to-noise ratio. Data from experiment 9 were misleading since the space probe was beginning its coming into the stratosphere.

Experiment number	Time segment (s)	Amplitude A (mm)	Frequency f (Hz)	Velocity V (cm s^{-1})	Acceleration Γ
1	23–36	0.1	3	0.2	0.004
2	46.8–52	2.5	1	1.6	0.01
3	52.3–67.3	2.5	3	4.7	0.09
4	76.5–84.5	0.3	30	5.6	1.1
5	87–100	0.1	60	3.8	1.4
6	103–116.5	0.3	60	11.3	4.3
7	120–130	1	60	37.7	14.5
8	138.5–148	2.5	30	47.1	9
9	151–180	2.5	60	94.2	36.2

its head is pointed perpendicular towards the pressure sensor surface. Typical pressure sensor characteristics are a 0.72 mV/Pa output sensitivity, a 20 Pa/g acceleration sensitivity, a 40 kHz resonant frequency, and a 8 μs rise time. The component of the pressure signals due to the sensor sensitivity to acceleration has been removed by signal processing using Fourier transforms. The firing of the engine, the stabilization of the rocket on its parabolic trajectory, and the despinning of the rocket lasts roughly 90 s, the apex being 150 km above the Earth. Then, the output signals of acceleration and pressure sensors are transferred to Earth in real time with a 2 kHz sampling rate during the 200 s of low gravity environment (about $10^{-5}g$) before the parachute opens, the first 20 s of the experiment being without vibration to let the granular medium relaxing.

The three vessels are displayed in Fig. 1 at two different phases of the vibration cycle: Fig. 1(a) [respectively, Fig. 1(b)] corresponds to a maximum "upward" (respectively, "downward") velocity (see also Fig. 2). The density is decreasing from the left to the right. In the most dilute case, the particles move erratically and their distribution is roughly homogeneous in space (there is a depletion close to the boundary moving away from the particles). In the two denser cases, a motionless dense cluster in the reference frame of the camera, i.e., of the space probe (black central region of the photographs) is surrounded by lower particle density regions. The spheres surrounding the cluster are in motion, mainly in the part of the vessel close to the boundary moving toward the granular medium. We thus observe that, at high enough density, the spatially homogeneous gas of particles undergoes an instability which leads to the formation of a dense cluster. Note that the left and the middle (respectively, right) cells are illuminated from the left (respectively, right) side. The apparent increase in cluster size is an artifact due to light diffusion (see Fig. 1).

The difference between the two kinetic regimes, homogeneous and clusterized, is also apparent on the pressure signals displayed in Fig. 2. In the dilute case (upper curve in Fig. 2), the time recording of the pressure, measured at the top wall (see Fig. 1), shows a succession of peaks corresponding to particle collisions with the wall. In the two denser cases, the pressure involves a component in phase with the acceleration imposed to the vessel (lower curve in Fig. 2). Note that, in the case of intermediate density

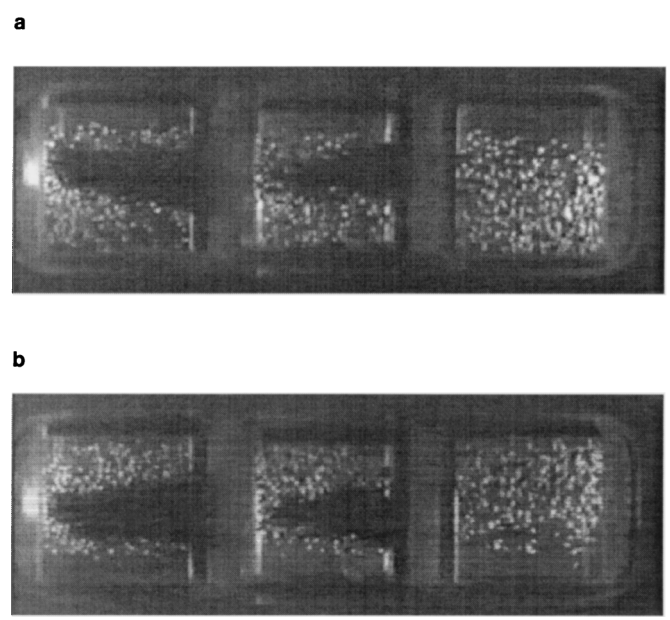

FIG. 1. From right (dilute cell) to left (densest cell): Transition from a dissipative granular gas to a dense cluster at two different phases of the vibration cycle in quadrature with the acceleration (see Fig. 2); (a) maximum "upward" velocity, (b) maximum "downward" velocity. On these pictures, a pressure sensor is on the "top" of each cell (not visible). The parameters of vibration are the ones of experiment No. 8 in Table I.

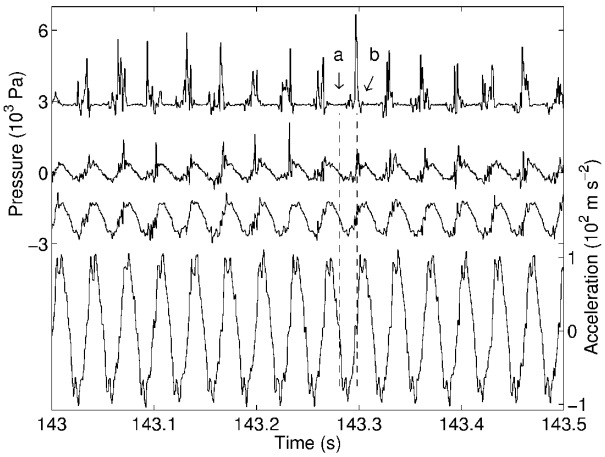

FIG. 2. From the lower to the upper curve: Time recordings of the acceleration in the direction of vibration, of the pressures in the densest cell, in the intermediate one, and in the dilute one. Letters a and b refer to the times when pictures in Figs. 1(a) and 1(b) have been taken. The parameters of vibration are the ones of experiment No. 8 in Table I. Pressure curves are shifted vertically for clarity.

(second signal from the top), both the pressure peaks and the component in phase with the acceleration are visible. However, the amplitude of pressure fluctuations is smaller than for the dilute case, although the particle number is larger; the reason is that most particles are in the cluster, which, as can be seen in the video recordings, stays away from the walls except for the largest amplitude of vibration. The pressure component, in phase with the acceleration, traces back to the grains in the low density region between the cluster and the walls. It shows that, in the densest case, the motion of these particles is coherent with the vibration, as already observed in numerical simulations [19]. In the case of intermediate density, the vibration generates both a coherent pressure oscillation and incoherent motions displayed by the random pressure peaks in the signal.

We now consider the dilute case for which the spatially homogeneous fluidized regime is stable. Particles move erratically and the pressure signal displays a succession of peaks. Note that the pressure being measured on the whole surface of the "top wall," a peak does not correspond to the collision of a single sphere, which would lead to an impact duration of about 2 μs [20] and is hardly resolvable by the transducer. These peaks correspond to a collective collision leading to a much longer typical impact duration of about 2 ms (thus resolved by the 2 kHz sampling rate). Bursts of peaks occur roughly in quadrature with the acceleration but the number of peaks in each burst, their amplitude, and the duration of each burst are random (see Fig. 2). Note the small distortions in the acceleration signal, occurring at the same times as the pressure peaks. The distortions near the extrema of the acceleration signal are generated by the mechanical driver at full stroke. Assuming a roughly homogeneous particle distribution, one can estimate that each peak in the pressure recording of Fig. 2 involves about 150 collisions. This shows that the mean duration between successive collisions is comparable to the transducer rise time. Besides, the probability of multiple collisions within the duration of a single collision is small. Thus, we do not expect the transducer response to be biased by multiple collisions along its surface within a short time period. As said above, the pressure signal in Fig. 2 is averaged on a time interval long compared to the duration of a single collision. It is thus proportional to the sum of the impulses of the successive collisions. Consequently, it depends on the mass and the incident velocities of the particles, but also on the elastic properties of both the particle and the transducer through the restitution coefficient.

Figure 3 displays the probability density functions of pressure fluctuations in the dilute case for various parameters of vibration. These probability density functions roughly scale like $V^{3/2}$, where V is the maximal vibration velocity of the vessel (V ranges from 1.6 to 47 cm s^{-1}). This $V^{3/2}$ scaling is more precisely observed on the standard deviation of the pressure signal (inset of Fig. 3).

Although pressure has been measured in previous experiments on coherent granular flows [2,3], it has surprisingly not been used to quantify incoherent "gaslike" kinetic regimes. Indeed, it is a much easier quantity to measure experimentally than granular temperature and, for a spatially homogeneous density, one expects their mean values to be proportional. The $V^{3/2}$ scaling for the pressure histograms thus implies a similar scaling for the granular temperature.

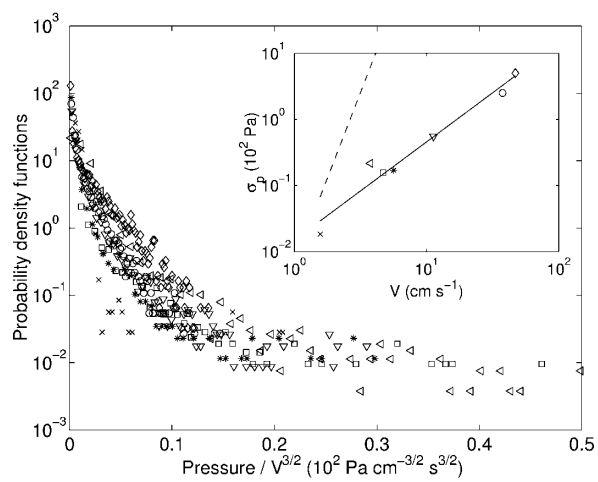

FIG. 3. Probability density functions of pressure fluctuations in the dilute cell rescaled by $V^{3/2}$ ($V = 2\pi A f$), for different vibrational parameters as in Table I experiment No. 2 (×); 3 (□); 4 (∗); 5 (◁); 6 (▽); 7 (○); 8 (◇). The inset displays the standard deviation $\sigma_p \equiv \sqrt{\langle (p - \langle p \rangle)^2 \rangle}$ of pressure fluctuations p versus V. Power law fit of the form $V^{3/2}$ (full line) and V^2 (dashed line).

Using dimensional analysis, the granular temperature, i.e., the mean kinetic energy per particle, E/N, scales like

$$\frac{E}{N} = mf^2A^2F\left(\epsilon, N, \frac{A}{L}, \frac{R}{L}\right), \qquad (1)$$

where m is the mass and F is an arbitrary function of R, the radius of the particles, L, the length of the vessel, ϵ, the restitution coefficient, A and N. Note that one should take into account different restitution coefficients for the particle-particle and the wall-particle collisions, but that this does not modify the frequency dependence of the granular temperature. Consequently, in low gravity, one expects the granular temperature or the mean pressure to be proportional to the square of the vibration frequency. This is not compulsory in the presence of gravity because an additional dimensionless parameter Af^2/g is involved in Eq. (1). Indeed, a previous experiment [7], numerical simulations [8–10], kinetic theory [7,12,21] and hydrodynamic models [11], all involving gravity, have found different scaling laws for the granular temperature, in the range $V^{4/3}$–V^2.

Our measurements in low gravity imply that another dimensionless parameter involving a new velocity scale should be considered in Eq. (1). The dependence of the restitution coefficient on the impact velocity provides this additional parameter. In our velocity range, the restitution coefficient varies from 0.97 to 0.87 as the velocity is increased [22]. Dissipative effects thus increase with velocity which leads to a smaller increase of the granular temperature with velocity than for a constant restitution coefficient. To be more specific, one can combine the result of kinetic theory, $E/N \propto V^2/(1 - \epsilon)$ with a viscoelastic model for the restitution coefficient, $1 - \epsilon \propto V^\alpha$ [20] to explain that the scaling exponent of the granular temperature as a function of the velocity is smaller than 2.

In conclusion, we have reported a 3D experiment of a granular medium fluidized by sinusoidal vibrations in low gravity environment. When the density of the granular medium is increased, we clearly show that an ensemble of particles in erratic motion interacting only through inelastic collisions spontaneously generates the formation of a motionless dense cluster.

We thank S. Aumaître for discussions. This work has been supported by the European Space Agency (France) and the Centre National d'Études Spatiales (France). The flight has been provided by E.S.A. The experiment module has been constructed by D.A.S.A. (Germany), Ferrari (Italy), and Techno System (Italy). *Mini-Texus 5* sounding rocket is a program of E.S.A. We gratefully acknowledge the Texus team for its kind technical assistance. E. F. was supported by a postdoctoral grant from the C.N.E.S.

*Corresponding author.
Email address: falcon@lps.ens.fr

[1] M. O. Faraday, Philos. Trans. R. Soc. London **52**, 299 (1831); J. Walker Sci. Am. **247**, No. 3, 166 (1982); P. Évesque and J. Rajchenbach, Phys. Rev. Lett. **62**, 44 (1989); B. Thomas and A. M. Squires, Phys. Rev. Lett. **81**, 574 (1998).
[2] C. Laroche, S. Douady, and S. Fauve, J. Phys. (Paris) **50**, 699 (1989).
[3] S. Douady, S. Fauve, and C. Laroche, Europhys. Lett. **8**, 621 (1989).
[4] S. Fauve, S. Douady, and C. Laroche, J. Phys. (Paris), Colloq. **50**, C3-187 (1989).
[5] P. B. Umbanhowar, F. Melo, and H. L. Swinney, Nature (London) **382**, 793 (1996).
[6] J. T. Jenkins and S. B. J. Savage, Fluid Mech. **130**, 187 (1983); C. S. Campbell, Annu. Rev. Fluid Mech. **22**, 57 (1990).
[7] S. Warr, J. M. Huntley, and G. T. H. Jacques, Phys. Rev. E **52**, 5583 (1995).
[8] S. Luding *et al.*, Phys. Rev. E **49**, 1634 (1994).
[9] S. Luding, H. J. Herrmann, and A. Blumen, Phys. Rev. E **50**, 3100 (1994).
[10] S. McNamara and S. Luding, Phys. Rev. E **58**, 813 (1998).
[11] J. Lee, Physica (Amsterdam) **219A**, 305 (1995).
[12] V. Kumaran, Phys. Rev. E **57**, 5660 (1998).
[13] P. Goldreich and S. Tremaine, Annu. Rev. Astron. Astrophys. **20**, 249 (1982).
[14] A. Kudrolli, M. Wolpert, and J. P. Gollub, Phys. Rev. Lett. **78**, 1383 (1997).
[15] S. Fauve, E. Falcon, and C. Laroche, CNES Report No. 95/0256, 1996 (unpublished).
[16] M. A. Hopkins and M. Y. Louge, Phys. Fluids A **3**, 47 (1991); S. McNamara and W. R. Young, Phys. Fluids A **4**, 496 (1992); I. Goldhirsch and G. Zanetti, Phys. Rev. Lett. **70**, 1619 (1993).
[17] F. G. Bridges, A. Hatzes, and D. N. C. Lin, Nature (London) **309**, 333 (1984).
[18] H. H. Shen, W. D. Hibler, and M. Leppäranta, J. Geophys. Res. **92**, 7085 (1987).
[19] S. McNamara and J. L. Barrat, Phys. Rev. E **55**, 7767 (1997).
[20] E. Falcon, C. Laroche, S. Fauve, and C. Coste, Eur. Phys. J. B **3**, 45 (1998).
[21] J. M. Huntley, Phys. Rev. E **58**, 5168 (1998).
[22] C. V. Raman, Phys. Rev. **12**, 442 (1918); W. Goldsmith, *Impact* (Arnold, London, 1960).